Metallophysics and Advanced Technologies
Металофіз. новітні технол.
Metallofiz. Noveishie Tekhnol.
2024, vol. 46, No. 3, pp. 211–221
https://doi.org/10.15407/mfint.46.03.0211
Reprints available directly from the publisher

PACS numbers: 61.46.Hk, 61.50.Lt, 61.72.jd, 68.35.bd, 71.15.Mb, 71.20.Be

Determinism of Gold-Monolayers' Local Atomic Ordering in the Formation of Their Electronic Structure

V. L. Karbivskyy, A. O. Romanskyy, A. P. Soroka, I. V. Sukhenko, V. Kh. Kasyanenko, L. I. Karbivska, and V. V. Stonis

G. V. Kurdyumov Institute for Metal Physics, N.A.S. of Ukraine,
36 Academician Vernadsky Blvd.,
UA-03142 Kyiv, Ukraine

The total and partial densities of electron states of layered gold structures of different symmetry with thickness from 1 to 10 monolayers are calculated within the framework of the density functional theory. As shown, the first co-ordination sphere is determinant in the formation of the fine structure and the extent of the valence bands of the monolayer gold structures. The splitting of the peaks of the TDOS curve, which leads to its finer structure, is influenced not only by the lengths of interatomic bonds, but by the mutual arrangement of atoms too. The influence of long-range interactions on the electronic structure of gold monolayers is established. For example, for the (110) plane, a change in the atomic ordering in the third co-ordination sphere as a result of the introduction of a vacancy leads to noticeable changes in the TDOS curve that indicates either a significant role of the atoms of the third co-ordination sphere, or a significant redistribution of the interaction of *d*-orbitals of different symmetries of close neighbours. A correlation between the packing density as well as the number of neighbours in the first co-ordination sphere and the width of the energy bands of gold monolayers is revealed.

Key words: metal monolayers, electron structure, DFT, crystal defects, chemical bonds.

У рамках теорії функціоналу густини (ТФГ) розраховано повну та парціяльні густини електронних станів шаруватих структур золота різної симе-

Corresponding author: Anastas Romanskyy
E-mail: anromansky@gmail.com

Citation: V. L. Karbivskyy, A. O. Romanskyy, A. P. Soroka, I. V. Sukhenko, V. Kh. Kasyanenko, L. I. Karbivska, and V. V. Stonis, Determinism of Gold-Monolayers' Local Atomic Ordering in the Formation of Their Electronic Structure, *Metallofiz. Noveishie Tekhnol.*, **46**, No. 3: 211–221 (2024). DOI: 10.15407/mfint.46.03.0211

трії товщиною від 1 до 10 моношарів. Показано, що перша координаційна сфера є визначальною у формуванні тонкої структури та ширини валентних зон моношарових структур золота. На розщеплення піків кривої повної густини станів, що приводить до більш тонкої структури, впливають не тільки довжини міжатомових зв'язків, але й взаємне розташування атомів. Встановлено вплив далекосяжних взаємодій на електронну структуру моношарів золота. Наприклад, для площини (110) зміна атомового порядку в третій координаційній сфері в результаті введення вакансії приводить до помітних змін на кривій повної густини станів, що свідчить або про значну роль атомів третьої координаційної сфери, або про істотний перерозподіл взаємодії d-орбіталей різних симетрій, що належать близьким сусідам. Встановлено кореляцію між щільністю пакування, а також кількістю сусідів у першій координаційній сфері та шириною енергетичних зон моношарів золота.

Ключові слова: металеві моношари, електронна структура, ТФГ, кристалічні дефекти, хемічні зв'язки.

(Received 1 September, 2023; in final version, 10 December, 2023)

1. INTRODUCTION

In Ref. [1], the change in the electron density of gold slabs in the (111) plane was studied as a function of the film thickness and defect concentration. The (111) plane was chosen due to the fact that monolayer gold films have the symmetry of the (111) plane [2–4]. The study of monolayers of other planes can provide extremely important information on the patterns of formation of features of the electronic structure of both thin gold films and bulk metal, and the study of the effect of defects on this process substantially supplements the systematic data on the formation of a general picture of the design of the electronic structure of metals of the gold group.

Despite the fact that the free existence of metal monolayers is doubtful from the point of view of solid-state physics, some features of the electronic structure in the presence, for example, of defects, could still allow the stable existence of such structures under certain conditions. In particular, our earlier experimental data [2–3] show that the formation of monolayer gold flakes in the presence of vacancies and stacking faults is still possible. In addition, it is important to take into account the fact that according to a number of works, in particular, [5–6], gold has a unique propensity for the stability of relatively large $2D$ clusters due to $5d$–$6s$ hybridization.

In addition, a theoretical study of the features of the electronic structure of metal monolayers, in particular, gold, is a necessary step for studying the regularities of the layer-by-layer growth of metallic nanostructures.

Today, the study of the properties and possibilities of using both

layer-by-layer grown nanostructures and thin gold films is extremely important, in particular, in electronics [7, 8], energetics [9], plasmonics and the creation of metamaterials [10–12].

The mechanisms for the formation of nanostructures of gold, as well as of its small clusters, still require a number of additions, although today there is already a very impressive array of data.

Inspired by the extremely important modern results, in particular, in Refs. [5, 13], this work is intended to supplement the data on the formation of the electronic structure of clusters and defective monolayers of gold, and is also caused by the desire of the authors to link the electronic-energy structure of gold monolayer structures with the initial physicochemical data of gold atoms and their topology on the plane.

2. RESEARCH METHOD

The total and partial densities of electronic states were obtained by the tetrahedron method [14] using Wien2k package [15, 16]. We used the full-potential (L)APW + lo method [17, 18] and generalized gradient approximation (GGA) PBE (Perdew, Burke, Ernzerhof), as the most common GGA functional [19]. The visualization of the atomic structure was carried out using VESTA [20].

3. RESULTS AND DISCUSSION

The obtained curves of the total density of electronic states (TDOS) of gold monolayers are shown in Fig. 1 and are arranged according to the degree of decrease in the packing density of atoms (Table 1). In addition, in the same row, there is regularity in the decrease in the number of neighbours in the first co-ordination sphere. At a distance of 2.88 Å, for monolayers of planes (111), (100), and (110), the number of atoms in the first co-ordination sphere is 6, 4, and 2, respectively.

Considering the nearest environment of atoms in relation to the features of the electronic structure, it is important to take into account not only the bond length, but also the specific position of the neighbour atom in the plane. For convenience, this position will be described by the angle φ (Fig. 2). Figure 2 shows the first three co-ordination spheres, because, in the case of a defective monolayer (110), changes in the atomic environment are observed only in the third co-ordination sphere.

In Ref. [1], changes in the TDOS curves of gold slabs in the (111) plane were analysed with a change in the number of monolayers and the presence of vacancies. It was shown that at certain vacancy concentrations in the monolayer of the (111) plane, the main maxima of the

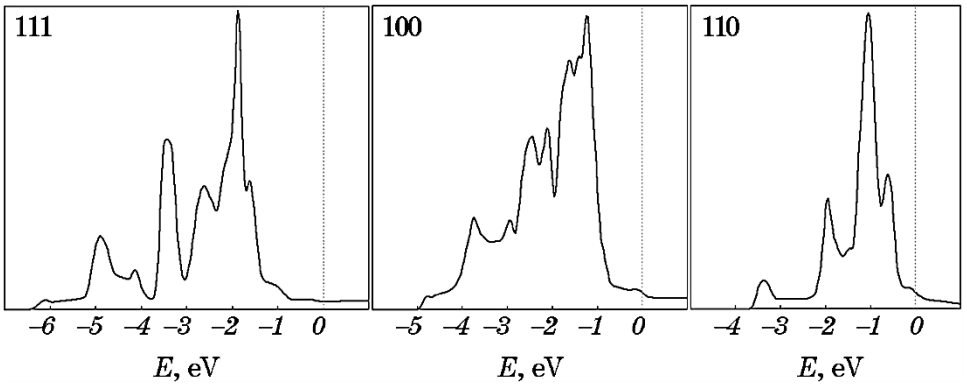

Fig. 1. Calculated TDOS of ideal monolayers of planes (111), (110), and (100).

TABLE 1. Energy position of the main maximum on the TDOS curve, interatomic-bond lengths and co-ordination numbers for different planes of gold monolayers.

Plane/cell area (Å²)/number of atoms per unit cell	(111)/ 8.29/ 1	(100)/ 16.65/ 2	(110)/ 11.75/ 1
Main maximum position (eV)	≅ 1.9	≅ 1.3	≅ 1.0
Bond lengths (Å)/co-ordination number	2.88/6 4.99/6 5.77/6	2.88/4 4.08/4 5.77/4	2.88/2 4.08/2 4.99/4
Atomic density (atom per nm²)	12.06	12.01	8.51

TDOS curve are split, which brings the shape of this curve closer to that for a bulk sample. Each atom of an ideal monolayer of gold in the (111) plane has six nearest neighbours in the first co-ordination sphere, which are characterized by an angle φ to the x axis, which affects different contributions from the d-state components.

As can be seen from Fig. 2 planes (110) and (100) have rotational symmetry different from (111). In view of this, the TDOS curves of gold monolayers of different planes have significant differences. A significant narrowing of the valence band is observed from ≅ 6.5 eV for a monolayer of the (111) plane to ≅ 3.5 eV for a monolayer of the (110) plane. Only three main features can be distinguished on the TDOS curve of the monolayer of the (110) plane. In contrast to the (110) plane, the gold (100) plane is characterized by the presence of an atom in the line segment connecting the central atom and the atom of the third co-ordination sphere (Fig. 2; r_3). However, the interatomic distances for the first and second co-ordination spheres for the (100) and

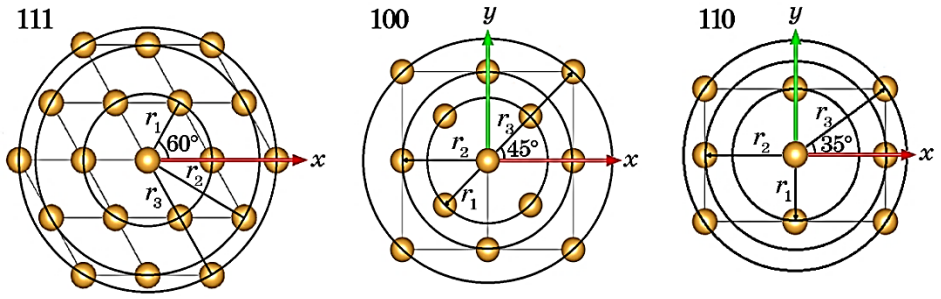

Fig. 2. The first three co-ordination spheres and the angle φ for gold monolayers of the (111), (100) and (110) planes.

(110) planes are of the same length. In the case of the (110) plane, the angles between the bond line and the coordinate axes differ only in the third co-ordination sphere; however, the distance of ≅ 5.0 Å is rather significant for bond formation and, accordingly, the contribution of the third co-ordination sphere to the TDOS curve should be extremely small.

It should be noted that with a different definition of the basis of the coordinate system, the angles of the corresponding bonds are still preserved; in this case, only the indices of the d-components change.

Consequently, significant differences in the TDOS curves for monolayers of the (100) and (110) planes are determined not only by the presence of two additional atoms at the distance of 4.08 Å for the (100) plane, but mainly by the different local symmetry that is characteristic of these planes.

When analysing the calculated data, an important criterion is their compliance with the experimental data. To assess the correctness of the obtained curves of the densities of electronic states, we carried out their comparative analysis with ultraviolet photoelectron spectroscopy (UPS) spectra. In particular, Figure 3 shows a comparison of the calculated curve of the total density of states for a gold slab containing three monatomic layers of the (110) plane and the spectrum of the valence band of gold in the (110) plane obtained by ultraviolet photoelectron spectroscopy [21].

It is known that the quantum-mechanical method used by us for calculating the electronic-energy structure tends to some energy compression of the obtained curves of electronic states. As can be seen from Fig. 3, with a slight stretching of the calculated curve, it can be argued that the main features of the density of electronic states are in full agreement.

Analysis of Fig. 4 allows us to assert that the main maximum of the density of electronic states is mainly formed by the d_{xz} and d_{z^2} electronic states. The peak to the right of the main peak at ≅ 0.5 eV owes its

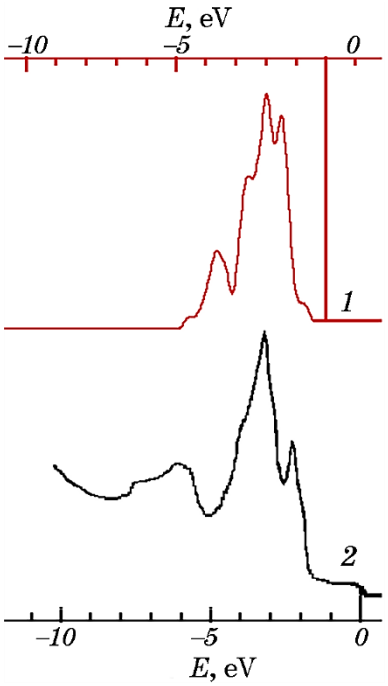

Fig. 3. Calculated TDOS curve for a gold slab containing 3 monatomic layers of the (110) plane (*1*) and UPS spectrum of clean gold surface of (110) plane [21] (*2*).

origin to d_{yz} and d_{xy} with an insignificant addition of $d_{x^2-y^2}$ states, which also participate in the formation of the main maximum. The feature to the left of the main maximum at about 2 eV is formed by the d_{yz} и d_{xy} states. The peak at 3.5 eV is determined by the $d_{x^2-y^2}$ states.

The transition to the analysis of the TDOS curve of the monolayer of the (100) plane shows a very rich fine structure of the valence band. The atomic density in such a monolayer in comparison with the (110) plane increases by almost 1.4 times. In the first co-ordination sphere at the same distance, there are no longer 2, but 4 atoms.

Based on the fact that for all the considered planes the first co-ordination sphere is at the same distance of 2.88 Å, and only the number of atoms in the co-ordination sphere changes (2, 4 and 6 respectively for the planes (110), (100) and (111)), it is obvious that the first co-ordination sphere is determinant in the formation of the fine structure and extent of the valence bands of the structures under study.

As shown earlier [1], in the case of the gold (111) plane, the contribution to the main maximum of the density of states is made mainly by the states associated with the z axis. For (110), this tendency remains, but, in addition to z^2, the xz component also makes a significant con-

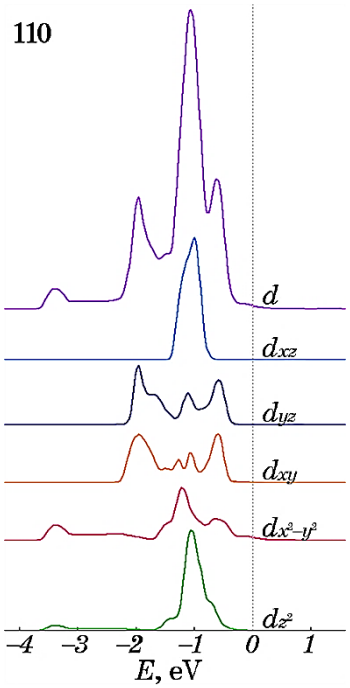

Fig. 4. Calculated partial contributions to the TDOS of an ideal gold monolayer of the (110) plane.

tribution. More precisely, only the d-states associated with the y axis have several significant peaks.

Thus, the complex band structure is formed by the bonds of the first co-ordination sphere. Moreover, the variability of the bond angles to the x and y axes determines the splitting of the peaks and the formation of a more complex band structure.

Since in the monolayer gold flakes studied by us earlier [2–3], due to defectiveness, the bond combinations are even more diverse, and, consequently, the TDOS curve has a more developed fine structure, the study of defective gold monolayers can be more applied than the calculations of ideal monolayers. Figure 5 shows the contributions of atoms of non-equivalent positions to the TDOS of the (110) plane defective monolayer (2×2 supercell).

Significant differences in the contributions to the TDOS between atoms of different positions are observed. The peak in the density of electronic states of the $Au_{(1)}$ atom forms a band with many features, similar in shape to the TDOS curve, but much less intense. This fact indicates an important role of the atoms of the first position in the formation of the structural features of the TDOS of the defect gold monolayer.

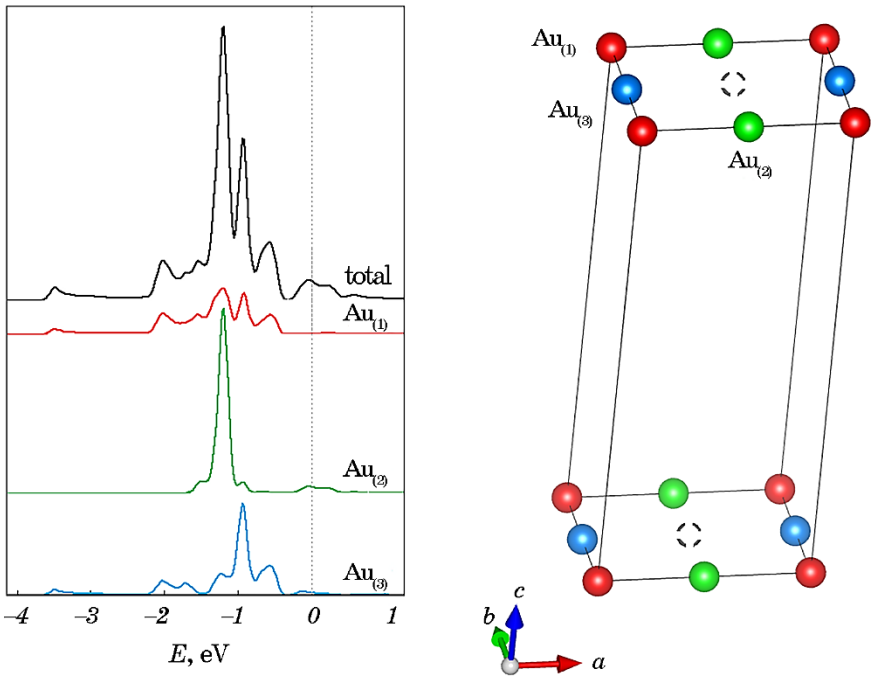

Fig. 5. Contributions of atoms from non-equivalent positions to TDOS of the (110) plane defective monolayer (2×2 supercell).

The intensity of the peaks on the curve of the density of states of the $Au_{(1)}$ atoms is lower than on the analogous curves of the $Au_{(2)}$ and $Au_{(3)}$ atoms. Most likely, this difference is caused by differences in the atomic environment. The atom of the first non-equivalent position does not contain defects in the first and second co-ordination spheres. Atoms of the second and third non-equivalent positions are adjacent to a vacancy and therefore, there is a break in bond with the nearest neighbour in one of the directions.

For atoms in the first position, it is extremely curious that changes in the atomic environment in this case are observed only in the third co-ordination sphere. Thus, although the nearest 2 co-ordination spheres do not undergo changes, the contribution of the densities of states of the $Au_{(1)}$ atoms to the TDOS undergoes changes. Consequently, sufficiently distant neighbours affect the density of states.

The curve of d-states of the $Au_{(2)}$ atoms has a very clear energy localization of about 1.2 eV, which corresponds to the position of the main maximum on the TDOS of the sample. Analysing the partial densities of d-states for atoms of each non-equivalent position, we can see that the intense peaks on the densities of states curves for $Au_{(3)}$ and $Au_{(2)}$ are determined, first of all, by the d-states associated with the x and y ax-

es.

In the presence of vacancies, the most significant differences between the TDOS curves of an ideal and a defective monolayer is, first of all, the appearance of a low-intensity feature in the region near the 'Fermi level'. The bond length between $Au_{(1)}$ and $Au_{(2)}$ along the x axis is quite large and amounts to 4.08 Å, while there are no neighbours along the y axis at a distance of $\cong$ 2.88 Å. In view of this, the atom of the second position, as can be seen in Fig. 6, is most sensitive to changes.

For the $Au_{(1)}$ atom, the splitting of the main peak of the d_{z2} states is observed. With a vacancy defectiveness of 2×2, $Au_{(1)}$ does not lose its neighbours from the first ($\cong$ 2.88 Å) and second ($\cong$ 4.08 Å) co-ordination spheres; however, it loses all neighbours from the third co-ordination sphere at once. Considering that this is the only change in its environment, it must be assumed that changes in the density of states curves for $Au_{(1)}$ are associated either with the interaction with atoms of the third co-ordination sphere, or with a change in the hybridization of various orbitals with neighbours in the first co-ordination sphere.

In the (110) plane defective monolayer, an insignificant band broad-

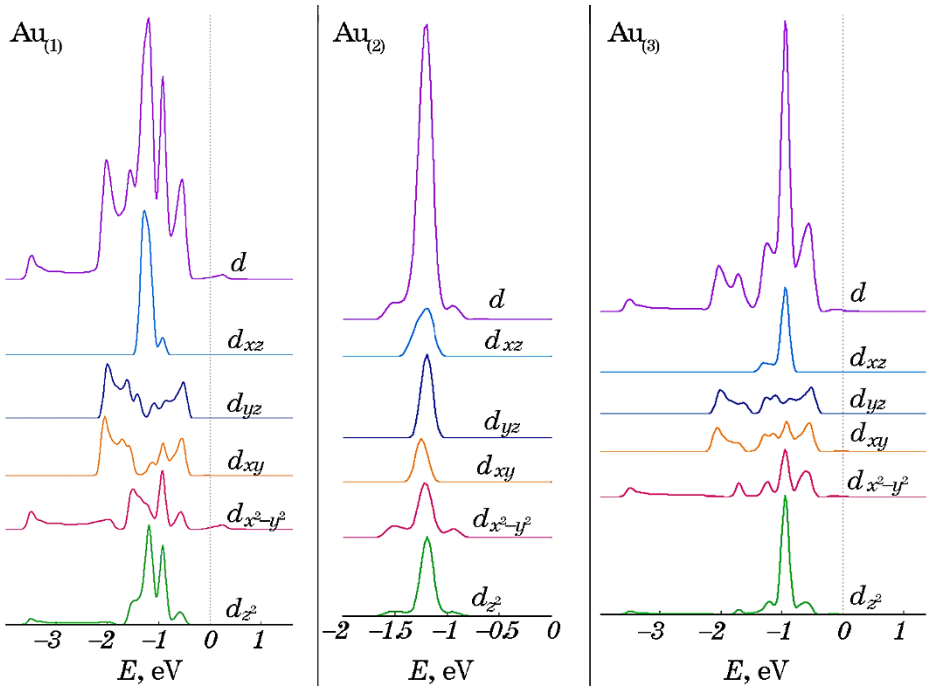

Fig. 6. Calculated partial densities of electronic states of the (110) plane defective monolayer.

ening is observed, due to the contributions of the d-states associated mainly with the y axis (in the chosen basis). Since in this case the shorter $Au_{(1)}$–$Au_{(3)}$ bond lies exactly on the y axis, it can be assumed that the broadening of the band is caused by a stronger interaction with the nearest neighbours.

4. CONCLUSIONS

The first co-ordination sphere is determinant in the formation of the fine structure and the extent of the valence bands of the monolayer gold structures. The splitting of the peaks of the TDOS curve, which leads to its finer structure, is influenced not only by the lengths of interatomic bonds, but also by the mutual arrangement of atoms.

The presence of a long-range effect of the atoms of the third co-ordination sphere on the electronic structure of gold monolayers is shown. For example, for the (110) plane, a change in the atomic ordering in the third co-ordination sphere as a result of the introduction of a vacancy leads to noticeable changes in the TDOS curve, which indicates either a significant role of the atoms of the third co-ordination sphere, or a significant redistribution of the interaction of d-orbitals of different symmetries of close neighbours.

A correlation between the packing density, as well as the number of neighbours in the first co-ordination sphere, and the width of the energy band of gold monolayers has been established.

REFERENCES

1. V. L. Karbivskii, A. A. Romansky, L. I. Karbivska, and S. I. Shulyma, *Appl. Nanosci.*, **12**, No. 3: 781 (2021).
2. V. L. Karbivskyy, V. V. Vyshniak, and V. H. Kasiyanenko, *J. Adv. Microsc. Res.*, **6**, No. 4: 278 (2011).
3. V. Karbivskyy, L. Karbivska, and V. Artemyuk, *Nanoscale Res. Lett.*, **11**, No. 1: 69 (2016).
4. L. I. Karbivska, V. L. Karbivskii, A. A. Romansky, O. Y. Kuznetsova, P. O. Teselko, and V. A. Artemyuk, *2019 IEEE 39th International Conference on Electronics and Nanotechnology* (ELNANO), (2019).
5. H. Häkkinen, *Chem. Soc. Rev.*, **37**, No. 9: 1847 (2008).
6. F. Munoz, A. Varas, J. Rogan, J. A. Valdivia, and M. Kiwi, *Phys. Chem. Chem. Phys.*, **17**, No. 45: 30492 (2015).
7. C. Liu, Y. Tang, P. Huo, and F. Chen, *Mater. Lett.*, **257**: 126708 (2019).
8. G. Yi Jia, Q. Zhang, Z. Xian Huang, S. Bin Huang, and J. Xu, *Phys. Chem. Chem. Phys.*, **19**, No. 40: 27259 (2017).
9. A. Kato, M. Suyama, C. Hotehama, H. Kowada, A. Sakuda, A. Hayashi, and M. Tatsumisago, *J. Electrochem. Soc.*, **165**, No. 9: A1950 (2018).
10. R. Lemasters, C. Zhang, M. Manjare, W. Zhu, J. Song, S. Urazhdin, H.J. Lezec, A. Agrawal, and H. Harutyunyan, *ACS Photonics*, **6**, No. 11: 2600 (2019).

11. R. A. Maniyara, D. Rodrigo, R. Yu, J. Canet-Ferrer, D. S. Ghosh, R. Yongsunthon, D. E. Baker, A. Rezikyan, F. J. García de Abajo, and V. Pruneri, *Nat. Photonics*, **13**, No. 5: 328 (2019).
12. O. Guselnikova, P. Postnikov, R. Elashnikov, M. Trusova, Y. Kalachyova, M. Libansky, J. Barek, Z. Kolska, V. Švorčík, and O. Lyutakov, *Colloids Surf. A*, **516**: 274 (2017).
13. M. F. Matus and H. Häkkinen, *Small*, **17**, No. 27 (2021).
14. P. E. Blöchl, O. Jepsen, and O. K. Andersen, *Phys. Rev. B*, **49**, No. 23: 16223 (1994).
15. K. Schwarz, P. Blaha, and G. K. H. Madsen, *Comput. Phys. Commun.*, **147**, Nos. 1–2: 71 (2002).
16. P. Blaha, K. Schwarz, F. Tran, R. Laskowski, G. K. H. Madsen, and L. D. Marks, *J. Chem. Phys.*, **152**, Iss. 7: 074101 (2020).
17. E. Sjöstedt, L. Nordström, and D.J. Singh, *Solid State Commun.*, **114**, No. 1: 15 (2000).
18. G. K. H. Madsen, P. Blaha, K. Schwarz, E. Sjöstedt, and L. Nordström, *Phys. Rev. B*, **64**: 195134 (2001).
19. J. P. Perdew, K. Burke, and M. Ernzerhof, *Phys. Rev. Lett.*, **77**, No. 18: 3865 (1996).
20. K. Momma and F. Izumi, *J. Appl. Cryst.*, **44**, No. 6: 1272 (2011).
21. J. M. Gottfried, K. J. Schmidt, S. L. M. Schroeder, and K. Christmann, *Surf. Sci.*, **525**, Nos. 1–3: 197 (2003).